Magnetocaloric Effect and Critical Behavior of Ni_7Cu_3 Alloys

Jimei Niu
Guangzhou College
South China University of Technology
Guangzhou 510800, China
e-mail: jimeiniu@163.com

Jiliang Zhang
Department of Physics and Materials Science
City University of Hong Kong
Hong Kong, China
jiliangz@hotmail.com

Zhigang Zheng
School of Materials Science & Engineering
South China University of Technology
Guangzhou 510640, China
Corresponding authors e-mail: mszgzheng@scut.edu.cn

Abstract—The Ni_7Cu_3 alloy was prepared by arc-melting. The magnetic and magnetocaloric properties of alloys had been investigated. The Ni_7Cu_3 alloy was formed in a single phase with Cubic Ni-type crystal structure. The sample undergoes a second order magnetic phase transition from ferromagnetic (FM) to paramagnetic (PM) and its Curie temperature is 293.7 K. A maximum values of magnetic entropy change are found to be 1.3, 1.1, 0.8, 0.6 and 0.3 $J \cdot kg^{-1}K^{-1}$ under 5T, 4T, 3T, 2T and 1T respectively, which are comparable with some ferromagnetic materials, such as $Nd_{0.9}Dy_{0.1}Co_4Al$. The critical behavior around the transition temperature is investigated in detail, using both the standard Kouvel - Fisher procedure as well as the study of the field dependence of the magnetocaloric effect. The values of the exponents β and γ are 0.608 and 2.138 respectively, which are large than the value of pure Ni. Results indicate that there are long-range magnetic coupling for Ni_7Cu_3 alloy.

Keywords- Ni_7Cu_3 alloy; magnetic property; Magnetocaloric effect, critical behavior; magnetic entropy change

I. INTRODUCTION

The magnetic materials with large magnetocaloric effect (MCE) have attracted considerable attention for magnetic refrigeration applications. In recent years, MCE has been found in various intermetallic alloys, such as $Gd_5Si_2Ge_2$[1], $La(Fe,Si)_{13}$[2, 3], $MnAs_{1-x}Sb_x$[4], $MnFeP_{1-x}Si_x$[5], Ni-Mn-In[6] and amorphous alloys $Gd_{60}Co_{40-x}Mn_x$[7]. Much recently, Ni-Cu alloys have been paid more and more attention because of their interesting physical properties and functionalities such as magnetic recording media, magnetic sensors, giant magnetoresistance and microelectromechanical systems. Recent investigations of Ni-Cu alloys are also mainly focused on the synthesis methods, as sputtering, molecular beam epitaxy and electrodeposition, while little attention is paid to explore the possible functionalities, such as magnetocaloric effects. Previous theoretical and experimental investigations have confirmed that Ni-Cu alloys exhibite either anisotropic magnetoresistance (AMR) or giant magnetoresistance (GMR), indicating its electronic structure and magnetic domain can be tailored by extend magnetic field. Therefore, the NiCu alloy may be a good system to explore new-type functionalities. Also, NiCu alloy displays a ferromagnetic(FM) – paramagnetic(PM) phase transition as reported previously. The purpose of this investigation is to explore the magnetic properties and magnetocaloric effect of Ni-Cu alloys.

II. EXPERIMENTAL

The polycrystalline Ni_7Cu_3 alloy was prepared by arc-melting a mixture of pure Ni (99.95wt%) and Cu (99.9 wt%) in argon atmosphere. To ensure compositional homogeneity, the ingots were repeatedly melted at least four times. Before characterization, the ingots were wrapped in Ta foil and annealed at 500°C for 5 days. The structure of the samples was identified by Philips X'pert Pro MPD X diffractometer, using a monochromatized X-ray beam with nickel filtered Cu $K_{\alpha 1}$ radiation (1.54056 Å) generated at 40 kV and 30 mA. The temperature and magnetic field dependences of magnetization were measured by a physical properties measurement system (PPMS-9, Quantum Design Co.).

III. RESULTS AND DISCUSSION

Fig .1 shows the X-ray diffraction (XRD) patterns of Ni_7Cu_3 alloy. The sample was formed in a single phase with Cubic Ni-type crystal structure (space group Fm $\bar{3}$m/225), indicating that adding Cu does not change the structure of Ni. Also one can see from Ni-Cu phase diagram that Ni_7Cu_3 alloy is solid solution.

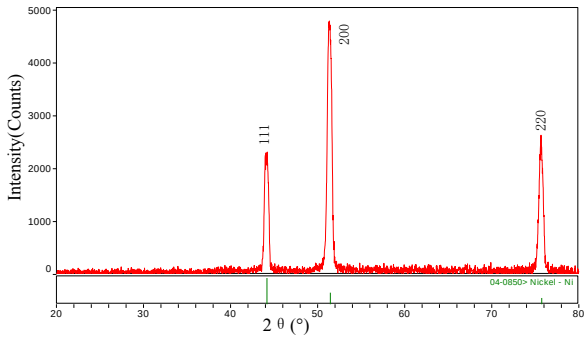

Figure 1. X-ray diffraction patterns of Ni7Cu3 alloy

The temperature (T) dependence of magnetization (M) of Ni_7Cu_3 alloy under a 1000 Oe applied field is shown in Fig .2. The Curie temperature T_C, which is defined as the temperature at the maximum of $|dM/dT|$ vs T plot, for Ni_7Cu_3 alloy is 293.7 K. The sample undergoes a ferromagnetic (FM) to paramagnetic (PM) order transition. The magnetization does not changes rapidly with the change of temperature in the vicinity of T_C, indicating that there is no large entropy change occured near Curie temperature. The inset of Fig .2 shows isothermal magnetization curves of the sample Ni_7Cu_3 in a temperature range of 229–349 K. The sweeping rate of the field was slow enough to ensure that the data were recorded in an isothermal process. The sample is saturated rapidly at lower field below their Curie temperature.

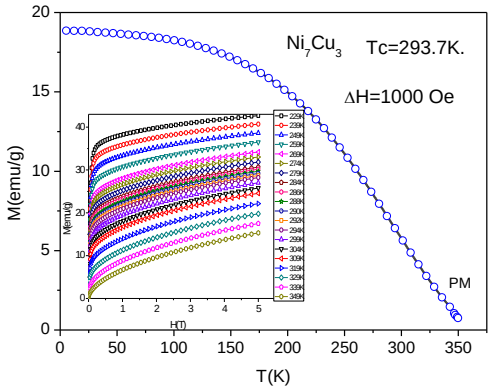

Figure 2. Temperature dependences of magnetization for Ni7Cu3 alloy under an applied field of 1000 Oe. The inset is isothermal magnetization curves as a function ofmagnetic field.

The magnetocaloric effects of Ni_7Cu_3 alloy were calculated in terms of isothermal magnetic entropy change by using Maxwell's equation. Fig .3 shows the temperature dependencies of $-\Delta S_M$ under the applied magnetic field change from 0 to 5 T. The peak values of $-\Delta S_M$ are found to be 1.3, 1.1, 0.8, 0.6 and 0.3 $J \cdot kg^{-1}K^{-1}$ under 5T, 4T, 3T, 2T and 1T respectively. It is comparable with these of some ferromagnetic materials, such as $Nd_{0.9}Dy_{0.1}Co_4Al$(0.8 $J \cdot kg^{-1}K^{-1}$ @ΔH=3T)[8], $GdCo_9Si_2$ (1.1 $J \cdot kg^{-1}K^{-1}$ @ΔH=5T)[9] and $Fe_{75}Nb_{10}B_{15}$ alloy(0.6 $J \cdot kg^{-1}K^{-1}$ @ΔH=1.5T)[10].

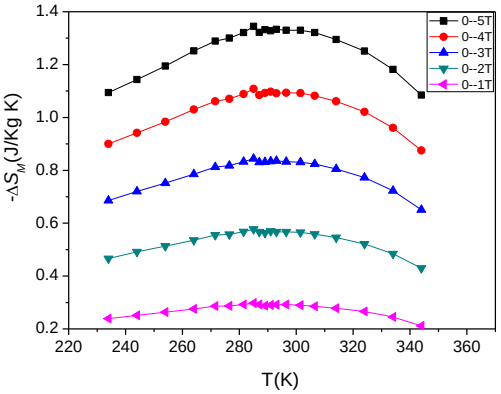

Figure 3. Magnetic entropy changes in Ni7Cu3 alloy under the magnetic field changes from 0 to 5 T

In order to study the magnetic phase transition of Ni_7Cu_3 alloy, the Arrott plot (H/M versus M^2) is depicted in Fig .4. It is widely accepted that the negative slopes or inflection points in the Arrott plots are related to first-order magnetic transition, while the positive slope and linear behavior near Tc often mean that the phase transition is second-order phase transition[7, 11]. Neither inflection nor a negative slope in the Arrott plot of Ni_7Cu_3 is observed near the T_C in Fig .4, which indicates that the alloy undergos a second-order magnetic transition.

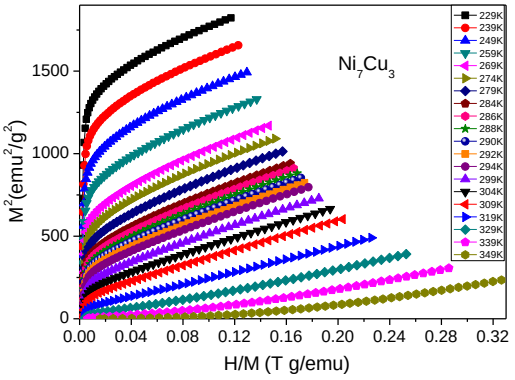

Figure 4. The Arrott plots of Ni7Cu3 alloy. The temperature step is 2 K in the vicinity of TC and 5 K in other ranges.

To analyze the nature of the magnetic phase transition in detail, we have carried out the study of the critical behavior near the Curie temperature T_C for the alloys. For the second-order magnetic phase transition, in the vicinity of Curie temperature T_C, the existence of a diverging correlation length $\xi=\xi_0(1-T/T_c)^{-\nu}$ leads to universal scaling laws for the spontaneous magnetization $M_S(T)$ and initial susceptibility $\chi(T)$. According to scaling hypothesis, the spontaneous magnetization $M_S(T)$ below T_C, the inverse initial susceptibility $\chi_0^{-1}(T)$ above T_C and the measured magnetization $M(H)$ at T_C are characterized by a set of critical exponents β, γ and δ, respectively. They are defined as:

$$M_s(0,T) = m_0|t|^{\beta} \qquad t \le 0 \qquad (1)$$

$$\chi_0^{-1}(0,T) = \frac{h_0}{m_0}|t|^{\gamma} \qquad t \ge 0 \qquad (2)$$

$$H = DM^{\delta} \qquad t = 0 \qquad (3)$$

where t is the reduced temperature ($t=T/T_C$-1), and m_0, h_0 and D are the critical amplitudes. Although the different critical exponents can be determined independently from experimental measurements, they are related to each other, which is taken in most cases to be of the form $\beta+\gamma=\beta\delta$. In order to properly determine the T_C, as well as the critical exponents β, γ, and δ, several methods can be used, including modified Arrott plots technique (MAPs), Kouvel–Fisher (KF) method and Widom scaling relation. For the Kouvel–Fisher method, two additional magnitudes are defined as:

$$Y(T) = -Ms(\frac{\partial Ms}{\partial T})^{-1} \qquad (4)$$

$$X(T) = \varphi^{-1}(\frac{\partial \chi^{-1}}{\partial T}) \qquad (5)$$

By plotting Y(T) and X(T) as a function of temperature, as shown in Fig .5, one should get straight lines around T_c with the slopes of -1/β and 1/γ, respectively, and the intercepts on the temperature axes are equal to T_c. The exponents obtained from KF method are as follows: β=0.608, γ=2.138 with T_c=292.8 K. The Tc is good agreement with experiment result, as shown in Fig .2. All these critical exponents are given in Table 1 along with the theoretically predicted values for different models, such as Mean-field theory, three-dimensional (3D) Heisenberg theory and three-dimensional (3D) Ising theory.

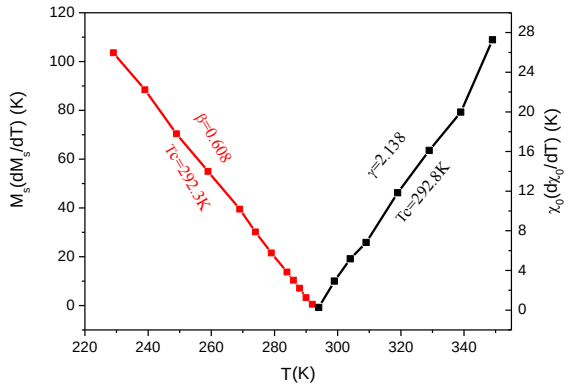

Figure 5. Y(T) and X(T) versus T for NiCu alloy

TABLE 1 The values of the exponents β, γ, and δ as determined from Kouvel-Fisher method for Ni_7Cu_3 alloy. The theoretically predicted values of exponents for various universal classes are also given for the sake of comparison.

Composition	T_c(K)	β	γ	δ	Ref.
Ni_7Cu_3	293.7	0.608	2.138	4.52	This work
Ni	627.4	0.378	1.34	4.58	[12]
Mean-field theory	-	0.5	1.0	3.0	[12]
Heisenberg theory	-	0.365	1.336	4.8	[12]
Ising theory	-	0.325	1.24	4.82	[12]

It should be noted that the 3D Heisenberg model or 3D Ising model is based on the short-range magnetic coupling, and mean-field theory is based on the long-range magnetic coupling. It is clear from Table 1 that, for Ni_7Cu_3 alloy the values of critical exponent β and γ increase fastly compared with pure Ni. The magnetic interactions in the present alloy exhibit long-range magnetic interactions. Physically, β describes how the ordered moment grows below T_C while γ describes the divergence of the magnetic susceptibility at T_C. The smaller the value of β, the faster is the growth of the ordered moment. The β value increases with increasing Cu contents, reflecting a slower growth of the ordered moment with decreasing temperature. This tendency is in agreement with magnetization intensity below T_c, which decreases with increasing non-magnetic Cu contents.

In the critical region, the magnetic equation of state can be written as:

$$M(H,t) = t^{\beta} f_{\pm}(H/t^{\beta+\gamma}) \qquad (6)$$

where $f_+(T>T_C)$ and $f_-(T<T_C)$ are the regular scaling functions[13]. In terms of renormalized magnetization $m = \frac{M(H,t)}{t^{\beta}}$ and renormalized field $h = \frac{H}{t^{\beta+\gamma}}$, Eq. (6) can be written as

$$m = f_{\pm}(h) \qquad (7)$$

Equation (7) implies that for true scaling relations and right choice of β, γ and δ values, scaled m plotted as a function of scaled h will fall on two universal curves: one above T_C and another below T_C. This is an important criterion for critical regime. As shown in Fig .6, the experimental data fall on two curves, one above T_C and the other below T_C, in agreement with the scaling theory. This result further indicates that the obtained values for the critical exponents and T_C are reliable.

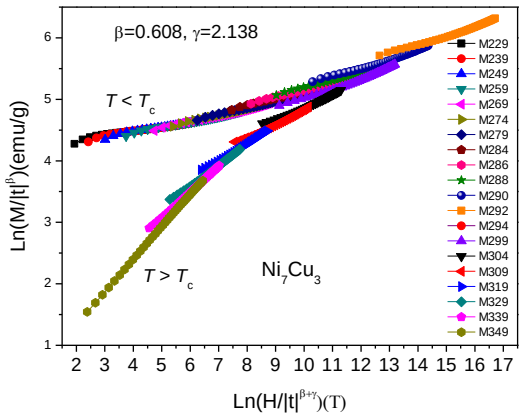

Figure 6. Scaling plots in a log–log scale below and above TC for Ni7Cu3 alloy β and γ determined by Kouvel-Fisher method

IV. CONCLUSION

The polycrystalline alloy Ni_7Cu_3 with Cubic Ni-type crystal structure (space group Fm $\bar{3}$m/225) was prepared by arc-melting. The magnetic and magnetocaloric properties of alloys have been investigated. It is interesting that the maximum value of $-\Delta S_M$ is 1.3, 1.1, 0.8, 0.6 and 0.3 $J \cdot kg^{-1}K^{-1}$ under 5T, 4T, 3T, 2T and 1T respectively. The Ni_7Cu_3 alloy exhibits second order magnetic phase

transition from FM to PM state. The critical exponent values determined by Kouvel-Fisher method are β=0.608, γ=2.138 with T_c=293.7 K, larger than the values predicted by the mean-field model, which have also been verified by the scaling equation of state. Furthermore, the critical exponents indicate that there are long-range magnetic coupling for Ni_7Cu_3 alloy.

ACKNOWLEDGMENT

This work is supported by Guangdong Provincial Science and Technology Program (Grant Nos. 2012B091000072), the Fundamental Research Funds for the Central Universities, SCUT (Grant No. 2014ZZ0005).

REFERENCES

[1] H. Fu, X. T. Zu, T. D. Shen. Structure and phase transformation of melt-spun Gd5Si2Ge2[J]. *Thermochimica Acta*. 2006, 445: 53-56.

[2] Zhiping Lin, Shandong Li, Su-Yueh Tsai, Jenq-Gong Duh, Meimei Liu, Feng Xu. The magnetic entropy change in La0.8Ce0.2Fe11.4Si1.6Bx compounds prepared by copper-mold casting[J]. *Journal of Magnetism and Magnetic Materials*. 2011, 323(13): 1741-1744.

[3] M. Zou, J. A. Sampaio, V. K. Pecharsky, K. A. Gschneidner. Spontaneous generation of voltage in the magnetocaloric compound La(Fe0.88Si0.12)13 and comparison to SmMn2Ge2[J]. *Physical Review B*. 2009, 80(17): 172403-172406.

[4] L. G. De Medeiros Jr, N. A. De Oliveira, A. Troper. Magnetocaloric and barocaloric effects in Mn(As0.7Sb0.3)[J]. *Journal of Magnetism and Magnetic Materials*. 2010, 322: 1558-1560.

[5] M. Hudl, P. Nordblad, T. Bj O Rkman, O. Eriksson, L. H A Ggstr O M, M. Sahlberg, Y. Andersson, E. K. Delczeg-Czirjak, L. Vitos. Order-disorder induced magnetic structures of FeMnP0.75Si0.25[J]. *Physical Review B*. 2011, 83(13): 134420.

[6] V. K. Sharma, M. K. Chattopadhyay, L. S. S. Chandra, S. B. Roy. Elevating the temperature regime of the large magnetocaloric effect in a Ni-Mn-In alloy towards room temperature[J]. *Journal of Physics D: Applied Physics*. 2011, 44(14): 145002-145006.

[7] Z. G. Zheng, X. C. Zhong, H. Y. Yu, V. Franco, Z. W. Liu, D. C. Zeng. The magnetocaloric effect and critical behavior in amorphous Gd60Co40-xMnx alloys[J]. *Journal of Applied Physics*. 2012, 111: 7A-922A.

[8] S. C. Ma, D. H. Wang, C. L. Zhang, H. C. Xuan, S. D. Li, Z. G. Huang, Y. W. Du. The study of the magnetic and room-temperature magnetocaloric properties in spin-reorientation Nd1-xDyxCo4Al (x = 0, 0.1) alloys[J]. *Journal of Alloys and Compounds*. 2010, 499: 7-10.

[9] Z. G. Zheng, X. C. Zhong, J. L. Zhang, Z. W. Liu, V. Franco, D. C. Zeng. Magnetic properties and magnetocaloric effects in GdCo9Si2 compound with multiple magnetic phase transitions[J]. *Journal of Applied Physics*. 2013, 113(17): 17A-938A.

[10] J. J. Ipus, J. S. Blázquez, V. Franco, A. Conde, L. F. Kiss. Magnetocaloric response of Fe75Nb10B15 powders partially amorphized by ball milling[J]. *Journal of Applied Physics*. 2009, 105: 123922-123927.

[11] Z. G. Zheng, X. C. Zhong, Z. W. Liu, D. C. Zeng, V. Franco, J. L. Zhang. Magnetocaloric effect and critical behavior of amorphous (Gd4Co3)1-xSix alloys[J]. *Journal of Magnetism and Magnetic Materials*. 2013, 343: 184-188.

[12] N. Khan, A. Midya, K. Mydeen, P. Mandal, A. Loidl, D. Prabhakaran. Critical behavior in single-crystalline La0.67Sr0.33CoO3[J]. *Physical Review B*. 2010, 82(6): 64422-64429.

[13] A. K. Pramanik, A. Banerjee. Critical behavior at paramagnetic to ferromagnetic phase transition in Pr0.5Sr0.5MnO3: A bulk magnetization study[J]. *Physical Review B (Condensed Matter and Materials Physics)*. 2009, 79: 214426-214432.